LAWRENCE
LIVERMORE
NATIONAL
LABORATORY

LLNL-TR-704799

Simulations of a Plasma Thruster Utilizing the FRC Configuration

T. D. Rognlien, B. I. Cohen

October 10, 2016

Disclaimer

This document was prepared as an account of work sponsored by an agency of the United States government. Neither the United States government nor Lawrence Livermore National Security, LLC, nor any of their employees makes any warranty, expressed or implied, or assumes any legal liability or responsibility for the accuracy, completeness, or usefulness of any information, apparatus, product, or process disclosed, or represents that its use would not infringe privately owned rights. Reference herein to any specific commercial product, process, or service by trade name, trademark, manufacturer, or otherwise does not necessarily constitute or imply its endorsement, recommendation, or favoring by the United States government or Lawrence Livermore National Security, LLC. The views and opinions of authors expressed herein do not necessarily state or reflect those of the United States government or Lawrence Livermore National Security, LLC, and shall not be used for advertising or product endorsement purposes.

This work performed under the auspices of the U.S. Department of Energy by Lawrence Livermore National Laboratory under Contract DE-AC52-07NA27344.

Simulations of a Plasma Thruster Utilizing the FRC Configuration

T.D. Rognlien and B.I. Cohen

Lawrence Livermore National Laboratory

1. Introduction

This report describes work performed by LLNL to model the behavior and performance of a reverse-field configuration (FRC) type of plasma device as a plasma thruster as summarized by Razin et al. [1], which also describes the MNX device at PPPL used to study this concept. Here neutral gas is fed into the open magnetic field-line region of the linear FRC device at one end, which is subsequently ionized by either large-orbit hot ions from the FRC that extend into the edge region or by electron cyclotron resonance heating. The energetic edge plasma produced then escapes out the opposite end, providing a net thrust. An experiment named MNX has been built and operated at PPPL to test this concept. A schematic of the configuration as taken from a PPPL slide is show in Fig. 1.

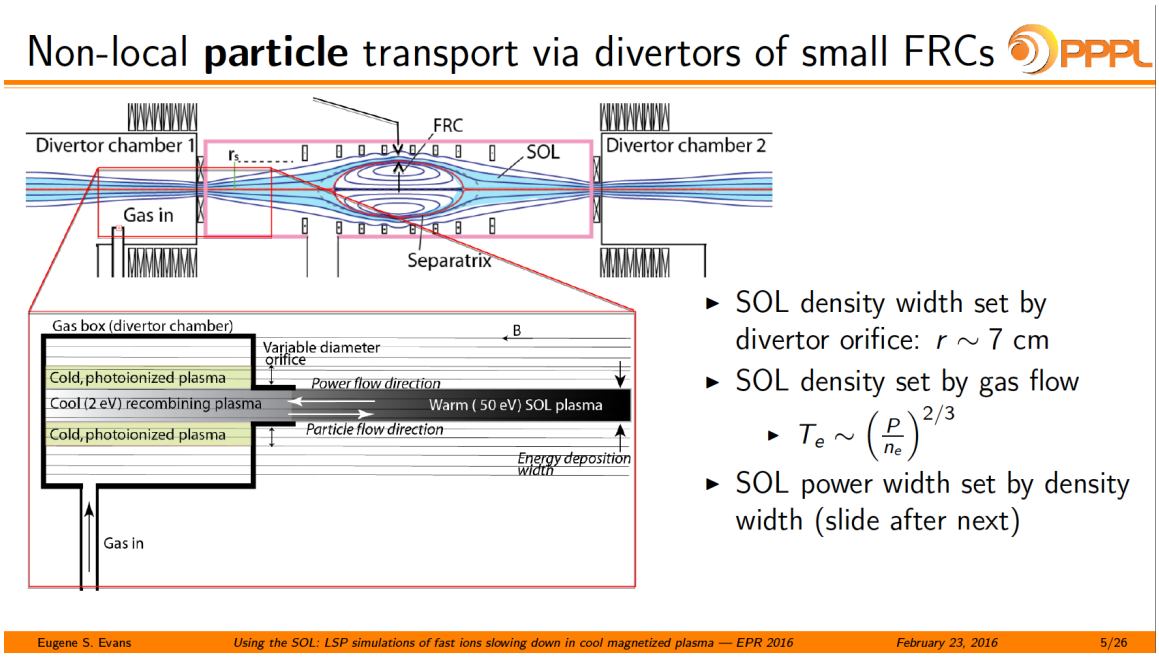

Fig. 1. Schematic of FRC thruster showing detail of the gas box injector on the left end.

In previous years we have modeled this concept with the UEDGE fluid plasma/neutral transport code in 1D and in a 2D slab model. This report covers the extension of those earlier studies to a realistic FRC-type of magnet geometry as show in Fig. 1. Over the course of the project, we have developed the geometry and code setup for various base-cases and then transferred that capability to students working at PPPL who performed more detailed parameter variables. A set of viewgraphs are appended to this report by Eugene Evans, a PPPL summer student from U. Penn., which shows the model work we facilitated in our recent extension to a 2D FRC configuration.

2. Model Magnetic MNX Field and Grid Used in UEDGE Simulations

A model magnetic field was generated for UEDGE simulation of the MNX experiment. A schematic of a typical Field Reversed Configuration (FRC) for the MNX thruster experiment is shown in Fig. 1. We have modeled this magnetic field configuration.

In the absence of plasma pressure and current profiles we cannot compute the self-consistent magnetic field profile from the magnetohydrodynamic equations. Instead we use analytic magnetic fields from dipole current loops using the textbook formulae[1] from magnetostatics for the applied mirror fields and shaping fields, and introduce a simple model magnetic field for the FRC. For each circular current loop with current I and radius a, the magnetic field (in c.g.s. units) is given by [1]

$$B_r = \frac{I\pi}{ac}\frac{3rza^3}{(a^2+r^2+z^2+2ar)^{5/2}} \qquad (1a)$$

$$B_z = \frac{I\pi a^2}{c}\frac{(2a^2+2z^2-r^2+ar)}{(a^2+r^2+z^2+2ar)^{5/2}} \qquad (1b)$$

where r=z=0 is relative to the center of the loop. The FRC magnetic field is represented by the following model axial field B_z with B_r constructed to satisfy div**B**=0 in a cylindrically symmetric system:

$$B_z = B_{0z} + \frac{2B_{FRC}(r-r_o)/L_r^2}{r\left(1+z^2/L_z^2\right)\left(1+(r-r_o)^2/L_z^2\right)^2} \qquad (2a)$$

$$B_r = \frac{-2B_{FRC}z/L_z^2}{r\left(1+z^2/L_z^2\right)^2\left(1+(r-r_o)^2/L_r^2\right)} \qquad (2b)$$

where r_o is the radius of the O-point in the FRC poloidal field, B_{0z} is the field strength of a uniform applied magnetic field, B_{FRC} is a parameter controlling the magnitude of the FRC magnetic field, $L_{r,z}$ are parameters controlling the radial and axial scale lengths of the FRC magnetic field, and r=r_o and z=0 in this representation locate the FRC O-point.

In our model magnetic field, we have two mirror magnetic coils placed outside the two throats ("magnetic nozzle points") symmetrically situated at the two ends of the FRC, a shaping coil over the FRC O-point, and an additional shaping coil outside the gas box section at the left. Field lines are traced by integrating Eq. (2) with a two-step predictor-corrector finite-difference scheme using linear interpolation of the

$$dr/B_r = dz/B_z \quad \Rightarrow \quad dr = B_r dz/B_z \qquad (3)$$

total magnetic field vector components in the two dimensions (r,z). In the gasbox region at the left end of the computational domain, the grid is given a higher resolution with smallest cell length along the field line $ds=(dz^2+dr^2)^{1/2}$ next to the left boundary, which cell length increases linearly to the end of the gasbox and then remains uniform over the remaining length of each field line. The radial spacing of the grid is uniformly distributed with respect to axial magnetic flux $\int B_z r dr$ at the left end of the system. A representative magnetic field is shown in Fig. 2 along with the corresponding field-aligned UEDGE grid constructed for the open-field-line scrape-off-layer of the MNX thruster system. The BASIS script used to construct the model magnetic field, compute its field lines, and generate the UEDGE grid shown in Fig. 2 is available on request. All magnetic fields are in Tesla, and lengths are in meters in the BASIS script.

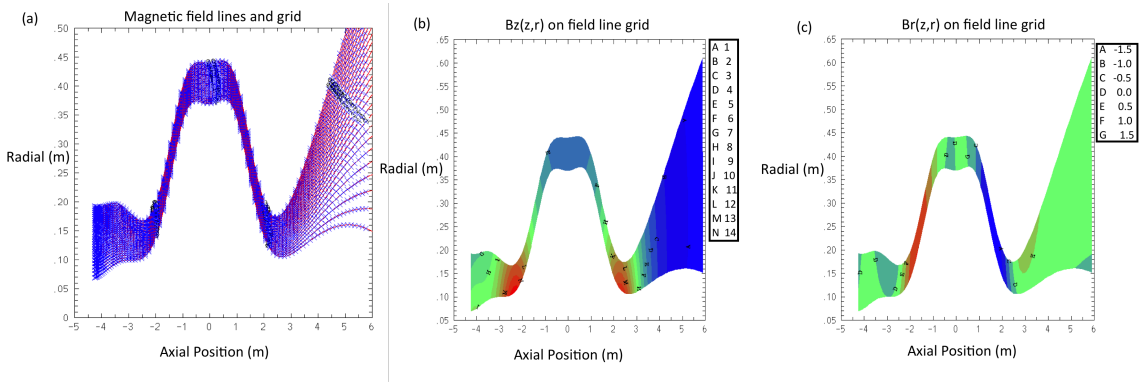

Fig. 2. (a) Field lines and grid cells; (b) B_z vs r,z ; (c) B_r vs r,z in the scrape-off-layer. There are 87 grid cells along each field line and 28 radial cells across the field lines.

3. UEDGE Model of the Plasma and Neutral Species

UEDGE is a 1D or 2D transport code that describes the magnetized-plasma/neutral species by a set of moment equations for species density, momentum, and energy. Transport along the magnetic field is taken from the Coulomb collisional model of Braginskii [3], while across the magnetic field anomalous diffusion coefficients are used to characterize the effect of plasma turbulence. Neutral transport is determined by collision processes among species and with ions and electrons. A full description of the model used in UEDGE together with some example simulations is given in Ref. 4. Details of geometrical and input options can be found in the UEDGE Users Manual. [5]

4. Examples of Transport Solutions

The simulations included here use deuterium plasma and include both atoms and molecules as neutral species. The anomalous plasma diffusivities are 0.5 m^2/s for ion density and 1.0 m^2/s for ion and electron temperatures, as well as ion viscosity. The magnetic geometry is that shown in Fig. 2, mesh sizes of 44x14 and 87x24 have been used with only small differences in the results.

The base case has a gas injection rate of 15 kA-equiv over a region within 1 m of the left boundary and a power into the electrons of 10 MW injected at the bottom of the magnetic well (0 on the axial position). The axial profiles are shown in Fig. 3

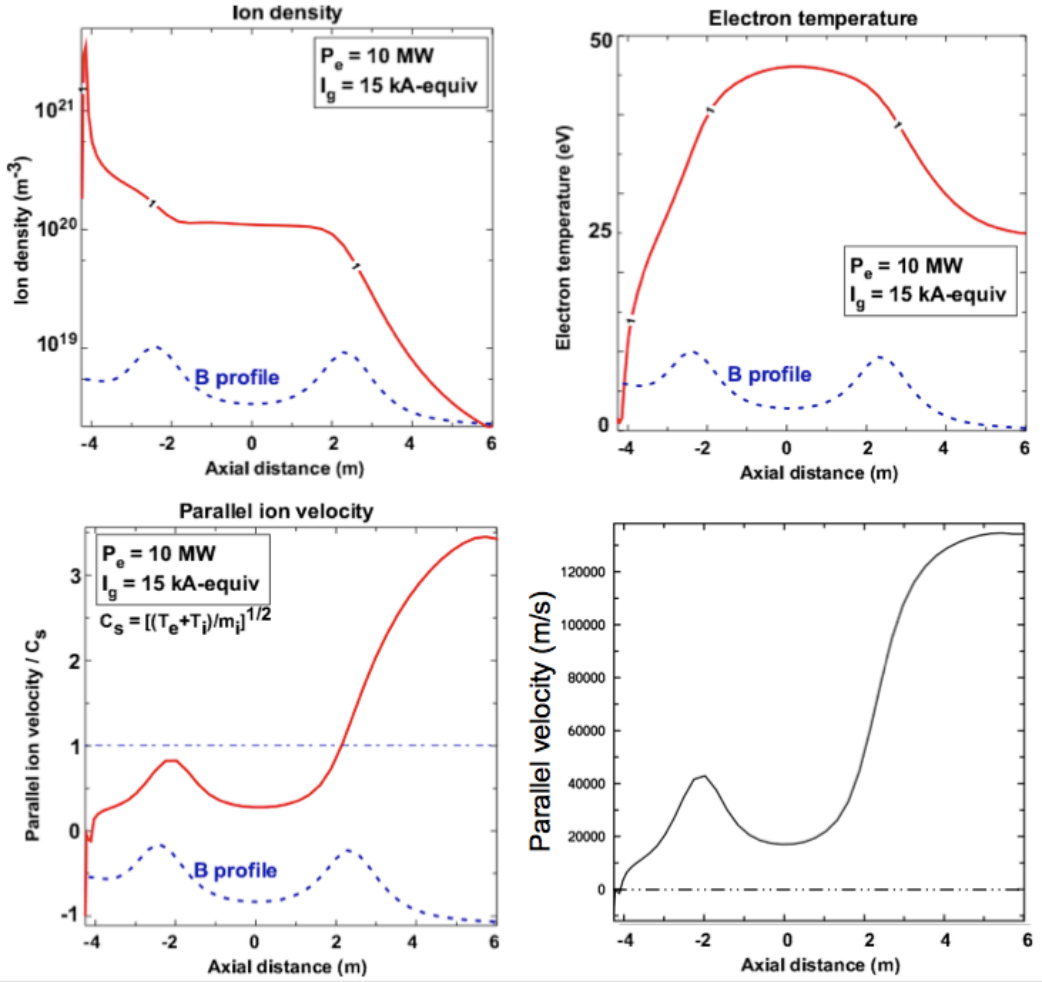

Fig. 3. Steady-state UEDGE profiles (moving clockwise from the upper left) for ion density, electron temperature, parallel ion velocity, and parallel ion velocity normalized to the ion-acoustic speed.

Note that the ion density is very large in the gas-box region near the left boundary and correspondingly the electron (and ion) temperatures are very low there – in the range of 1eV where strong plasma recombination can take place (a feature of detached plasmas operation in operation of tokamaks and other devices.). At the exit end to the right of the FRC, the ion density has dropped over two orders of magnitude.

The thrust caused by the injection of gas and power is of primary interest. We have scanned these two input parameters (gas injection rate and power into electrons) and show the results in Fig. 4. Here the red dot denotes the base case shown in Fig. 3. There is a saturation of the thrust as either parameter is extended much beyond this base case. Of course, there are many other variations possible; and some of these have been investigated by our co-investigators at PPPL and are not reported further here.

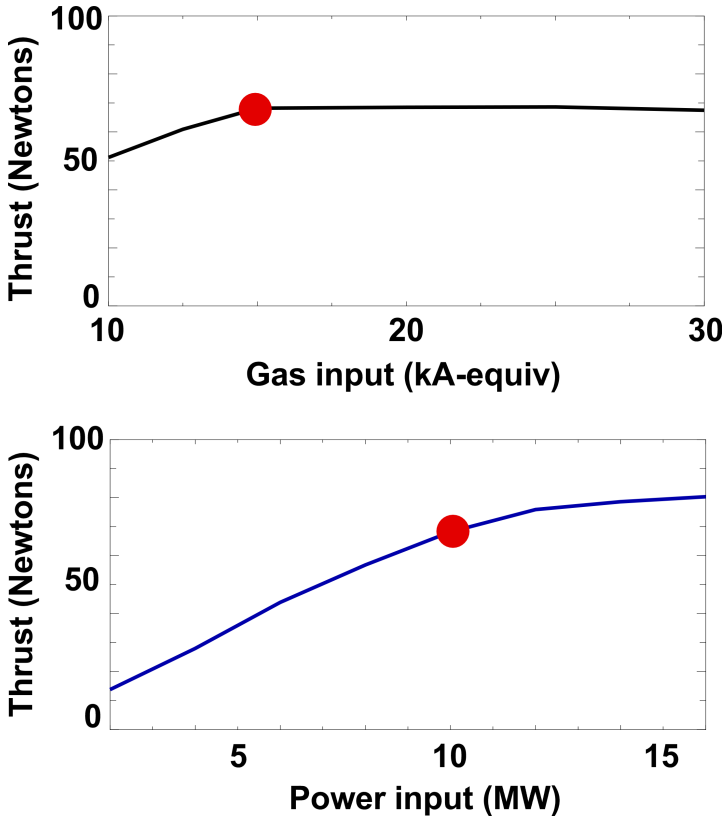

Fig. 4. Thrust out the right-hand boundary of the FRC configuration of Fig. 2 as input gas and electron heating power are varied. The red dot corresponds to the conditions for the base case shown in Fig. 3.

5. Summary

The UEDGE capability to simulate the plasma thruster based on the FRC concept has been extended to a 2D magnetic mirror geometry. Initial simulations show that there are optimal values of the gas injection and power input to produce the highest thrust. Both the UEDGE code and the geometry generating scripts, together with base-case input files have been given to PPPL. Consultation has been provided on an as-needed basis.

Acknowledgements

This work was performed under the auspices of the U.S. Department of Energy by Lawrence Livermore National Laboratory under contract DE-AC52- 07NA27344. This material is based upon work supported by the U.S. Department of Energy, Office of Science, Office of Fusion Energy Sciences.

References

1. Y.S. Razin, G. Pajer, M. Breton et al., "A direct fusion drive for rocket propulsion," Acta Astron. **105** (2014) 145.

2. J.D. Jackson, *Classical Electrodynamics*, (Wiley & Sons, New York, 1962), Sec. 5.5.
3. S.I. Braginskii, Transport processes in a plasma, in: M.A. Leontovich (Ed.), *Reviews of Plasma Physics*, vol. 1, (Consultants Bureau, New York, 1965), p. 205.
4. T.D. Rognlien and M.E. Rensink, "Edge-plasma models and characteristics for magnetic fusion energy devices," Fusion Eng. Design **60** (2002) 497.
5. T.D. Rognlien, M.E. Rensink, G.R. Smith, User Manual for the UEDGE Edge-Plasma Transport Code, LLNL Report, UCRL-ID-137121, 2008.